POLITECNICO DI TORINO
Repository ISTITUZIONALE

Noise-induced phenomena in riparian vegetation dynamics

Original
Noise-induced phenomena in riparian vegetation dynamics / Camporeale, CARLO VINCENZO; Ridolfi, Luca. - In: GEOPHYSICAL RESEARCH LETTERS. - ISSN 0094-8276. - STAMPA. - 34:(2007), pp. L18406-1-L18406-4. [10.1029/2007GL030899]

Availability:
This version is available at: 11583/1654284 since:

Publisher:
AGU

Published
DOI:10.1029/2007GL030899

Terms of use:
openAccess

This article is made available under terms and conditions as specified in the corresponding bibliographic description in the repository

Publisher copyright
AGU

Da definire

(Article begins on next page)

18 August 2022

GEOPHYSICAL RESEARCH LETTERS, VOL. 34, L18406, doi:10.1029/2007GL030899, 2007

Click Here for Full Article

Noise-induced phenomena in riparian vegetation dynamics

C. Camporeale[1] and L. Ridolfi[1]

Received 8 June 2007; revised 17 August 2007; accepted 24 August 2007; published 29 September 2007.

[1] Random forcing due to the river streamflow is a key element in riparian vegetation ecosystems. It influences several aspects of the riparian landscape, the most important being the morphology and water availability. In this letter, we analytically solve a stochastic model to show how hydrological random fluctuations are able to induce both statistically stable states and bimodality in vegetation behavior. These noise-induced results can contribute to explain two well-documented features of several riparian landscapes: the bell-shaped biomass distribution along riparian transects, and spatial vegetation patchiness along a river. **Citation:** Camporeale, C., and L. Ridolfi (2007), Noise-induced phenomena in riparian vegetation dynamics, *Geophys. Res. Lett.*, *34*, L18406, doi:10.1029/2007GL030899.

[2] In recent years, the role of noise-induced phenomena in ecosystems has attracted a great deal of interest in the scientific community [*Horsthemke and Lefever*, 2006]. Random changes in environmental conditions and disturbance regimes are not only sources of disorder, but can also induce new behavior in ecosystem dynamics. Two of the most interesting noise-induced phenomena are (1) the emergence of an intermediate statistically stable configuration between the two preferential states of the deterministic dynamics [*D'Odorico et al.*, 2005], and (2) the coexistence of more preferential states in the ecosystem [*Porporato and D'Odorico*, 2004]. Both these phenomena are particularly relevant from an ecological point of view. In the first case – called noise-induced stability – random external forcing prevents ecosystem from reaching a deterministic stable state, and the ecosystem fluctuates around a more probable intermediate state. In the second case, the ecosystem continually switches between two (or more) different states with rapid transitions through (unlikely) intermediate states.

[3] In this work we suggest that both forms of noise-induced phenomena may emerge in the dynamics of riparian vegetation. Riparian vegetation is a fundamental component of riparian ecotones, which are known for their environmental and ecological value, due to their complex bio-morphological and ecological dynamics, and their ability to provide habitat for several animal populations [*Malanson*, 1993]. This explains why, in recent years, a great deal of effort has been devoted to studying riparian vegetation environments, whose fragility makes them a very sensitive indicator of human-induced environmental changes [*Naiman et al.*, 2005].

[4] A key element of a riparian ecosystem is the variability of the fluvial hydrological regime [*Tockner et al.*, 2000]. The problem can be schematized as in Figure 1a, which shows the generic shape of a river cross-section. The random evolution of the discharge, $Q(t)$ – which depends on many hydrological components – induces variations in both the water level, $h(t)$, and the phreatic surface position, $\zeta(x, h)$ (where t is the time and x is the transversal coordinate). As a consequence, $h(t)$ and $\zeta(x, h)$ are stochastic variables themselves whose probabilistic characteristics depend on those of the discharge and on the local hydraulic and geometric characteristics of the river and the groundwater. As riparian vegetation greatly relies on river-controlled water availability and it suffers from flooding, it follows that the vegetation dynamics are forced by the stochastic nature of the fluvial regime to a great extent. Several field investigations have testified such a crucial hydrological influence. For example, flooding conditions are able to induce anoxia [*Kozlowski*, 1984], uprooting [*Osterkamp and Costa*, 1987], and burial [*Friedman and Auble*, 1999], while drought periods induce an elevated lowering of the aquifer water table thus inducing high water stress.

[5] Recently, some eco-hydrological models that take into account random discharge fluctuations have been proposed for riparian vegetation dynamics [e.g., *Brookes et al.*, 2000]. However, these are often conceptual qualitative models and at present the impact of river-induced randomness mostly remains poorly understood [*Lytle and Merritt*, 2004]. In particular, the emergence of noise-induced phenomena has never been explored. In this work, we adopt a stochastic model that we have recently proposed and whose results agree with real data [*Camporeale and Ridolfi*, 2006], to show that hydrological fluctuations are able to drive both noise-induced stability and noise-induced bimodality in vegetation biomass dynamics along a riparian transect with a possible link to the *intermediate disturbance hypothesis* [e.g., *Bendix*, 1997].

[6] We refer to the overall vegetation biomass of phreatophyte riparian species, neglecting interspecific interactions and geomorphological processes, such as sedimentation and erosion, namely a steady river morphology [*Auble et al.*, 1994]. Moreover, timescale considerations make it possible to ignore the time delay between the vertical movements of the free surface in the river and the water level in the adjacent unconfined aquifer beneath the vegetation. Under these hypotheses, we have shown [*Camporeale and Ridolfi*, 2006] that the local stochastic dynamics of the dimensionless density biomass, v, of single-species riparian vegetation can be modeled according to the following dichotomic process

$$\frac{dv}{dt} = \begin{cases} -\alpha v^n & h \geq \eta \\ v^m(\beta - v)^p & h < \eta, \end{cases} \tag{1}$$

[1]Dipartimento di Idraulica, Politecnico di Torino, Turin, Italy.

Copyright 2007 by the American Geophysical Union.
0094-8276/07/2007GL030899$05.00

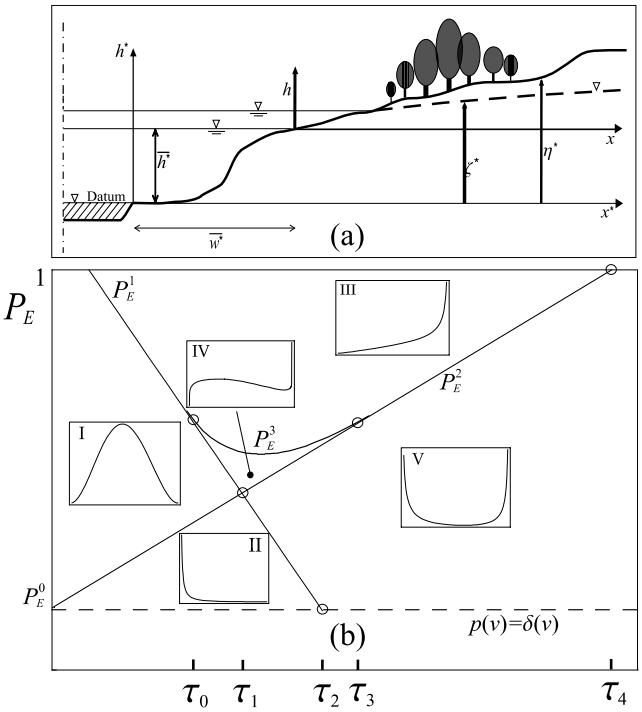

Figure 1. (a) Sketch of the riparian transect and main variables adopted. The star marks the dimensioned variables, while the dimensionless variables are normalized using the average values of the level, $\overline{h}^*$, and the river width, $\overline{w}^*$; therefore $x = x^*/\overline{w}^* - 1$, $h = h^*/\overline{h}^* - 1$, $\zeta = \zeta^*/\overline{h}^* - 1$, and $\eta = \eta^*/\overline{h}^* - 1$. (b) Scenario of the possible shapes of the vegetation biomass pdf, $p(v)$, depending on the exposure probability, P_E, and the correlation time scale, τ.

with

$$\alpha = \frac{\langle \alpha_1 \rangle}{\alpha_2} = k\langle h - \eta \rangle = \frac{k}{P_I}\int_{\eta(x)}^{\infty} (h - \eta)p(h)dh, \tag{2}$$

$$\beta = \langle V_c \rangle = \frac{1}{P_E}\int_{-1}^{\eta(x)} V_c p(h)dh, \tag{3}$$

$$V_c = V_c(\delta) = \begin{cases} 1 - a(\delta - \delta_{opt})^2 & \delta_1 \le \delta \le \delta_2 \\ 0 & \delta < \delta_1, \quad \delta > \delta_2. \end{cases} \tag{4}$$

Equation (1a) models the decay of the vegetation biomass caused by flooding and assumes that the eventual beneficial influences are overcome by the detrimental processes (i.e., anoxia, burial, uprooting, etc.). The coefficient α_1 is assumed to be an increasing function of h, as the mechanical effect of the stream water on vegetation is proportional to the tangential stress on the bed [*Friedman and Auble*, 1999], while anoxic conditions increase with the water level. Therefore, equation (2) models $\alpha_1 = K(h - \eta)$ where $K = \alpha_2 k$ is a species-dependent positive empirical coefficient and $\eta(x)$ is the dimensionless topographic elevation.

[7] Equation (1b) is a generalization of the commonly used Verhulst-logistic function that simulates the growth of a phreatophyte species tapping the groundwater [*Botkin et al.*, 1972]. The function $V_c = V_c(\delta)$ is the dimensionless carrying capacity (i.e., the maximum sustainable biomass) which depends on the depth of the aquifer water table, $\delta \equiv \eta - h$, through the quadratic optimum function (4), as suggested by *Phipps* [1979]. Finally, P_I and P_E are the probabilities of inundation and exposure of the plot, whereas the dimensionless time t is scaled according to $t = \alpha_2 t^*$. Due to its versatility, equation (1b) is able to fit several vegetation growth model laws well [*Camporeale and Ridolfi*, 2006].

[8] The statistical characteristics of the dichotomic switching in equations (1a–1b) are described by the probability distribution, $p(h)$, and the correlation time scale, $\tau = \alpha_2 \tau^*$, of the water level time series, the latter quantity being representative of the memory of the hydrological forcing.

[9] Model (1) can be written as a single stochastic differential equation driven by multiplicative dichotomic noise [*Kitahara et al.*, 1980]. The solution of the corresponding Fokker-Plank equation is the pdf of the vegetation density $p(v, t)$ with a steady state solution which, for the case $n = m = p = 1$, reads

$$p(v) = \frac{N}{\alpha} v^{\frac{\beta(1-\alpha\tau)-(\alpha+\beta)P_I}{\alpha\beta\tau}} (\beta - v)^{\frac{P_I}{\beta\tau}-1} (\alpha + \beta - v), \tag{5}$$

where $v \in [0, \beta]$, and N is the normalization constant. The above solution is valid provided $P_I < \beta/(\alpha + \beta)$, otherwise $p(v) = \delta(v)$, where $\delta(\cdot)$ is the Dirac delta function. In the following we refer to μ_v and σ_v as the mean and standard deviation of $p(v)$, respectively (for the algebraic expressions see *Camporeale and Ridolfi* [2006]).

[10] It is useful to begin the analysis of the role played by noise by considering the asymptotic behavior of $p(v)$ for $\alpha \to 0$ and $\alpha \to \infty$. The first limit is due to very weak flood events or a great resistance of the vegetation to the flood. In both cases, the vegetation decay becomes negligible with respect to the growth and the vegetation biomass evolves toward its maximum value, β. Accordingly, the limit of the steady pdf becomes $p(v) = \delta(v - \beta)$.

[11] Conversely, the limit $\alpha \to \infty$ occurs wherever the vegetation is very sensitive to the disturbance of the flooding, as well as when flooding is frequent and/or heavy. In this case, we obtain $p(v) = \delta(v)$.

[12] The previous asymptotic behavior helps us to understand the different qualitative scenarios that can be described by solution (5). Basically, when the inundation probability, P_I, and α, are very low, the disturbance is rare and well-resisted by the vegetation. Thus, a probability distribution that peaks at the carrying capacity β and decreases for smaller values can be expected. In this case, the only effect of the noise is to disturb the deterministic solution ($p(v) = \delta(v - \beta)$), but it does not introduce new modes. On the other hand, when stress conditions increase or the vegetation is less resistent, the pdf of the biomass gradually moves towards the opposite asymptotic behavior described by an atom of probability in $v = 0$. Finally, in intermediate conditions between the two asymptotic ones (the most usual case), $p(v)$ assumes a noise-induced unimodal shape characterized by different skewness levels

with a maximum located in the] 0-β [interval. This last pdf shape does not have a counterpart when noise is absent, and it is noise-induced.

[13] The structural change in the shape of the pdf can be recognized by exploring the signs of the first and the second v-derivatives of (5). In this way, three marginal curves that discriminate the domains of existence of the pdf shapes can be obtained. In the plane (τ, P_E), after introducing $\gamma = (\alpha + \beta)^{-1}$, such a curves read

$$P_E^{(1)} = 1 - \tau\beta, \quad P_E^{(2)} = 1 - \gamma\beta(1 - \tau\alpha), \quad P_E^{(3)} = \frac{4\alpha\tau^2 + \gamma}{4\tau}. \tag{6}$$

[14] Figure 1b plots the above curves along with the dashed line $P_E^{(0)} = \alpha\gamma$ which is derived from the condition of existence for solution (5), while the insets show the five different possible patterns of $p(v)$. In order to discuss this picture, let us consider the five increasing values of the correlation scale $\{\tau_0, \tau_1, \tau_2, \tau_3, \tau_4\} = \{\frac{\gamma}{2}, \frac{\gamma}{\gamma\alpha+1}, \frac{1}{2\alpha}, \gamma, \frac{1}{\alpha}\}$, which are marked by circles in Figure 1b. Both curves described by equations (6) and the latter temporal quantities $\{\tau_i\}$ depend on α and β and are therefore species-dependent.

[15] Firstly, when $P_E < P_E^{(0)}$, the vegetation biomass is identically equal to zero (i.e., $p(v) = \delta(v)$), regardless of the correlation scale. In fact, the site is too frequently flooded and the growth is continually inhibited. Then, moving from the dashed line according to an increasing probability of exposure, P_E, six scenarios can be recognized: (1) If $\tau \leq \tau_0$, three unimodal distributions can exist (II $\rightarrow$ I $\rightarrow$ III) where the maximum moves from zero to β when P_E increases. In this case, the correlation in the river discharge time series is low, therefore, bimodal distributions are impossible. Shape I is a remarkable example of noise-induced stability. (2) If $\tau_0 < \tau \leq \tau_1$, a small niche of bimodal pattern (shape IV) appears when P_E is between $P_E^{(1)}$ and $P_E^{(2)}$, thus the sequence becomes II $\rightarrow$ I $\rightarrow$ IV $\rightarrow$ III. It should be noticed that bimodal distribution IV has the lowest mode different from zero. (3) If $\tau_1 < \tau \leq \tau_2$, the two-peaked distribution V, namely the most drastic shape of bimodality with the modes in zero and β, appears in place of the regular one-peaked distribution I. In this case, phases with high biomass alternate with other almost unvegetated phases, and the mean value is no longer representative of the distribution, as it is a very low probable value. It should be noticed that this case differs from the switching between two alternative coexistent stable states (sensu *Scheffer et al.* [2001]). (4) If $\tau_2 < \tau \leq \tau_3$, the monotonic left-sided distribution II disappears and the niche of shape IV becomes thinner, therefore the sequence reduces to V $\rightarrow$ IV $\rightarrow$ III. (5) If $\tau_3 < \tau \leq \tau_4$, the first bimodal pattern also disappears (shape IV) and only two states remain possible: V and III. (6) Finally, if $\tau > \tau_4$, the only possible state is the bimodal distribution V.

[16] It is worthwhile observing that the condition for the emergence of the bimodal distribution V, namely $\tau > \tau_4$, in the dimensioned variables reads $\tau^* > (K\langle h - \eta\rangle)^{-1} \sim O(K^{-1})$ which does not depend on the growth parameters, but only on the decay characteristics of the plant. Hence, types of vegetation that report high values of K – i.e., with low resistance to uprooting, anoxia, burial or to the dynamic impact of the floods – provide a low value of the threshold τ_4^*, and are therefore more susceptible to bimodal behavior. If we consider the case $n = m = p = 1$, it can immediately be seen that $\alpha_2 \simeq 6/T_g^*$, where T_g^* is the characteristic timescale for the growth, defined as the time necessary for vegetation to undergo an overall growth of 90%. It follows that α_2 spans the range $[10^{-5} - 10^{-3}]$ for tree species and $[10^{-3} - 10^{-2}]$ for grass and shrubs. Considering that the correlation scale of the river flow varies between a few days to several months, we obtain that the dimensionless quantity τ spans the range $[10^{-5} - 10^{-1}]$ for trees and $[10^{-3} - 1]$ for grass and shrubs.

[17] Now let us consider the riverine section shown in Figure 2. This is a quasi-trapezoidal topography that is usually adopted to schematize a riparian transect. We reasonably assume a log-normal distribution of the flow, from which a standard Gamma distribution is derived to model the pdf, $p(h)$, of the water level in the river [*Camporeale and Ridolfi*, 2006], i.e., $p(h) = \Gamma(\lambda)^{-1}\lambda^{\lambda}(1 + h)^{\lambda-1}e^{-\lambda(1+h)}$, where $\lambda = 1/C_h^2$ and C_h is the coefficient of variation with realistic values being in the range [0.25, 0.75]. The insets 3(a)-(h) show the resulting vegetation biomass pdfs for two different species in four plots along the transect, and considering two different dimensional river correlation time scales τ_1^* and τ_2^*, with $\tau_1^* \ll \tau_2^*$. We choose a flooding-tolerant species (represented by the blue curves and indicated with $\mathcal{B}$), and a less tolerant species (species $\mathcal{R}$, red lines). The flooding-tolerance (i.e., low values of α) can be due both to a high resistance to the negative effects of floods (uprooting, anoxia, etc.), and to a high resilience, because of the short vegetation growth time scale; namely, low K and high α_2, respectively. The profiles of the mean, μ, and the standard deviation, σ, of the vegetation biomass are also shown in Figure 2.

[18] The behavior of the mean confirms that $\mathcal{R}$ is less tolerant to flooding than $\mathcal{B}$. Moreover, both species exhibit a maximum of μ along the transect; this behavior is often observable in real riparian ecosystems [e.g., *Johnson et al.*, 1995] and it is due to the detrimental effect of floods near the river and the decay of the aquifer water table far from the river. If the insets are compared vertically and a single species ($\mathcal{R}$ or $\mathcal{B}$) is focused on, it can be noticed that an increase in the correlation time does not significantly affect μ, but can drastically alter the shape of the pdfs, as can also be seen from the increase in the standard deviation, σ. It follows that the mean value might not be representative of the biomass dynamics, in particular when bimodal structures emerge. When the insets are compared horizontally, it is evident that the pdfs depend on the plot position along the transect to a great extent: not only the quantitative characteristics, but the shape itself can change, and different noise-induced phenomena can emerge along the same riparian transect and for the same species.

[19] When two (or even more) species coexist in the ecosystem, their different responses to the river forcing and the occurrence of noise-induced phenomena can give rise to several combinations of the pdf of each species and, in some cases, this can induce the emergence of spatial patchiness, although competition processes are not considered in this modeling. For example, in the cases described by insets (a) and (c), there is a dominance of species $\mathcal{B}$; it follows that species $\mathcal{B}$ invariably covers all the sites near the rivers with a small correlation time. Instead, farther from the river bank,

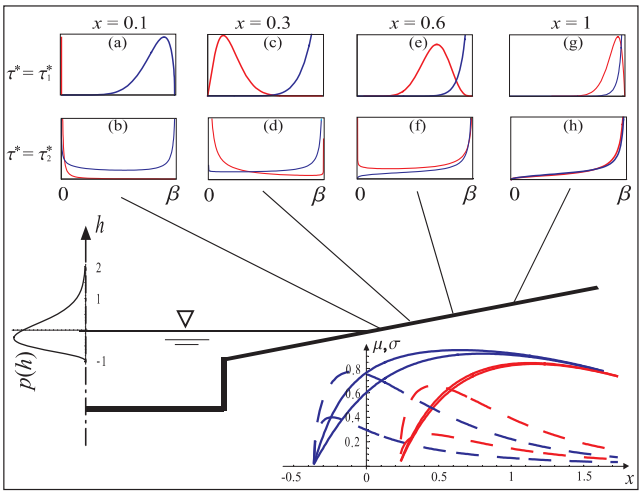

Figure 2. Probability density functions in four plots along a quasi-trapezoidal riparian transect. The solid and dashed lines show the mean and standard deviations along the transect, respectively. For the mean values, the upper curves refer to $\tau^* = \tau_1^* = 15$ days and the lower curves refers to $\tau^* = \tau_2^* = 180$ days, while for the standard deviation, the correspondence is inverted. ($C_h = 0.5$; $K = 0.01$; $\delta^* = 0.5$ m; $\overline{h}^* = 1.5$ m; $T_g^* \simeq 1$ year for the $\mathcal{B}$ species; $T_g^* \simeq 10$ years for the $\mathcal{R}$ species.)

in the insets (*e*), (*g*) and (*h*), both species perform distributions that peak at values close to the corresponding carrying capacity (i.e., β); a mixed coverage can therefore be expected. More complex and intriguing behavior is contained in the insets (*b*), (*d*) and (*f*) where the river flow is considered to be closely correlated. In this case, one or both distributions are in fact bimodal. This means that, among all the possible realizations, three scenarios are the most probable: (1) $v = \beta$ for both species; (2) $v = 0$ for both species; (3) $v = \beta$ for one species and $v = 0$ for the other one. In the first scenario, the result is a mixed coverage of the two species. In the second scenario, the result is basically bare ground. Finally, the third scenario gives the conditions for the emergence of patchiness. The latter conclusion can be explained by invoking a sort of ergodicity of the riparian vegetation dynamics. Different sites along the riparian corridor (but at the same distance from the river) in fact experience different realizations of the same stochastic process. Therefore, due to the random nature of the vegetation dynamics that allows species $\mathcal{R}$ to prevail in some realizations and species $\mathcal{B}$ to prevail in other realizations, it follows that some sites are dominated by $\mathcal{R}$ while other sites are dominated by $\mathcal{B}$, namely a patchy composition of the riparian zone.

[20] It is also worthwhile noticing that the previous picture can contribute to explain a community organization without the need to invoke niche differentiation. This is coherent with ecological studies that depict the riparian zone as a nonequilibrium system where the patches are continually redistributed in space and time because of disturbance linked to seasonal variability, individual storms and floods' [*Naiman et al.*, 2005, p. 163].

[21] To our knowledge, no field data are available concerning the temporal pdf of vegetation biomass, however, under the ergodic hypothesis, we can see in space and at a fixed time what we are not able to see in a plot over time. From this point of view, we suggest that the well-documented spatial patchiness along the river can also be considered as an important clue to bimodal behavior.

[22] We are aware that several processes that are not described by our model, such as intra- and inter-species competition, fires, erosion, sedimentation, and river migration [e.g., *Perucca et al.*, 2006], contribute to patchiness. However, we suggest that the alternation of flooding and exposure periods offers a further contribution to the formation of patchiness. Furthermore, it is well documented how the intermittent action of floods can hamper riparian vegetation biomass from reaching its potential maximum development [e.g., *Bendix and Hupp*, 2000]. This agrees with the outcome of our model, which shows clearly how river-induced noise is able to keep the vegetation system around an intermediate statistically stable state.

References

Auble, G. T., J. M. Friedman, and M. L. Scott (1994), Relating riparian vegetation to present and future streamflows, *Ecol. Appl.*, *4*(3), 544–554.

Bendix, J. (1997), Flood disturbance and the distribution of riparian species diversity, *Geogr. Rev.*, *87*(4), 468–483.

Bendix, J., and C. R. Hupp (2000), Hydrological and geomorphological impacts on riparian plant communities, *Hydrol. Processes*, *14*, 2977–2990.

Botkin, D. B., J. F. Janak, and J. R. Wallis (1972), Some ecological consequences of a computer model of forest growth, *J. Ecol.*, *60*, 849–872.

Brookes, C. J., J. M. Hooke, and J. Mant (2000), Modelling vegetation interactions with channel flow in river valley of the Mediterranean region, *Catena*, *40*, 93–118.

Camporeale, C., and L. Ridolfi (2006), Riparian vegetation distribution induced by river flow variability: A stochastic approach, *Water Resour. Res.*, *42*, W10415, doi:10.1029/2006WR004933.

D'Odorico, P., F. Laio, and L. Ridolfi (2005), Noise-induced stability in dryland plant ecosystems, *Proc. Natl. Acad. Sci. U. S. A.*, *102*(31), 10,819–10,822.

Friedman, J. M., and G. T. Auble (1999), Mortality of riparian box elder from sediment mobilization and extended inundation, *Reg. Rivers Res. Manage.*, *15*, 463–476.

Horsthemke, W., and R. Lefever (2006), *Noise-Induced Transitions*, 2nd ed., Springer, Berlin.

Johnson, W. C., M. D. Dixon, R. Simons, S. Jenson, and K. Larson (1995), Mapping the response of riparian vegetation to possible flow reductions in the Snake River, Idaho, *Geomorphology*, *13*, 159–173.

Kitahara, K. T., W. Horsthemke, R. Lefever, and Y. Inaba (1980), Phase diagrams of noise induced transitions, *Prog. Theor. Phys.*, *64*(4), 1233–1247.

Kozlowski, T. T. (1984), Responses of woody plants to flooding, in *Flooding and Plant Growth*, edited by T. T. Kozlowski, pp. 129–163, Academic, San Diego, Calif.

Lytle, D. A., and D. M. Merritt (2004), Hydrologic regimes and riparian forests: A structured population model for cottonwood, *Ecology*, *85*(9), 2493–2503.

Malanson, G. P. (1993), *Riparian Landscapes, Cambridge Studies Ecol.*, Cambridge Univ. Press, Cambridge, U. K.

Naiman, R. J., H. Decamps, and M. E. McClain (2005), *Riparia*, Elsevier, Amsterdam.

Osterkamp, W. R., and J. E. Costa (1987), Change accompanying an extraordinary flood on sandbed stream, in *Catastrophic Flooding*, edited by L. Mayer and D. Nash, pp. 201–224, Allen and Unwin, Boston.

Perucca, E., C. Camporeale, and L. Ridolfi (2006), Influence of river meandering dynamics on riparian vegetation pattern formation, *J. Geophys. Res.*, *111*, G01001, doi:10.1029/2005JG000073.

Phipps, R. L. (1979), Simulation of wetland forest dynamics, *Ecol. Modell.*, *7*, 257–288.

Porporato, A., and P. D'Odorico (2004), Phase transitions driven by state-dependent poisson noise, *Phys. Rev. Lett.*, *92*(11), 110601.

Scheffer, M., S. Carpenter, J. Foley, C. Folke, and B. Walker (2001), Catastrophic shift in ecosystems, *Nature*, *413*, 591–596.

Tockner, K., F. Malard, and J. V. Ward (2000), An extension of the flood pulse concept, *Hydrol. Processes*, *14*, 2861–2883.

C. Camporeale and L. Ridolfi, Dipartimento di Idraulica, Politecnico di Torino, Corso Duca degli Abruzzi 24, I-10129 Torino, Italy. (carlo.camporeale@polito.it)